

A practical approach to polarimetric adaptive target detection in Passive Radar

F. Filippini, F. Colone

*Dept. of Information Engineering, Electronics and Telecommunications (DIET),
Sapienza University of Rome
Via Eudossiana, 18 - 00184 Rome, Italy
{francesca.filippini, fabiola.colone}@uniroma1.it*

Keywords: Passive radars, target detection, polarimetric diversity, adaptive detection scheme

Abstract

Recently, the exploitation of polarimetric diversity was considered as a way to improve target detection capability in passive radar systems. Specifically, it was shown that a locally adaptive Polarimetric - Generalized Likelihood Ratio Test (P-GLRT) detection scheme might represent an effective solution for passive radar exploiting different signals of opportunity. However, depending on the considered application, it could be highly computationally expensive. The present work presents an alternative lower-cost approach, based on a global adaptation of the polarimetric whitening filter. The proposed scheme is tested against experimental data collected by means of a dual-pol receiving system. The reported analysis shows that it allows comparable performance with respect to the previously introduced approach, especially when operating against scenarios characterized by strong interfering sources.

1 Introduction

Passive Coherent Location (PCL) technology has been receiving conspicuous interest in the last decades yielding target detection and localization performance of passive radar to be steadily improved [1,2]. However, despite the effectiveness of the signal processing techniques developed for this purpose, the performance of a PCL system might be strongly limited by a variety of disturbance sources, other than the direct signal from the transmitter and its multipath replicas. With particular reference to a FM radio based PCL system, the major disturbance sources are represented by co-channel and adjacent-channel interferences [3], typically due to frequency reuse or broad-spectrum roll-off.

The possibility of combining the returns from differently polarized antennas has been recently considered as a way to improve the target detection capability against such disturbance. A first attempt toward this direction has been presented in [4] where a Non Coherent Integration (NCI) of the results obtained at two orthogonally polarized surveillance antennas was considered, based on the consideration that target echoes typically show a random polarization and the use of different polarizations on receive leads to different Signal to Interference plus Noise Ratio (SINR)[5].

A Polarimetric - Generalized Likelihood Ratio Test (P-GLRT) detection scheme was derived in [6] for a FM radio based PCL, able to adaptively exploit the polarimetric differences between the target and the competing disturbance (e.g. cancellation residuals or interfering signals).

The extensive analysis reported in [6] shows that, thanks to its capability to locally adapt the filter weights in the bistatic range-Doppler domain, the conceived P-GLRT scheme allows to successfully mitigate the effects of the interferences thus significantly improving the target detection performance of the system. In [7,8] similar conclusions have been drawn for a DVB-T based PCL system.

Clearly, depending on the application, a locally adaptive approach as the P-GLRT may result in a very high computational load required. Therefore, in this work, we look for an alternative approach able to provide a reasonable trade-off between achievable performance and computational complexity.

To this purpose, we investigate the possibility of globally adapting the weights of the polarimetric whitening filter by estimating the disturbance covariance matrix in the time domain. This requires the estimation and inversion of a single covariance matrix at each coherent processing interval (CPI) with a dramatic reduction of the computational burden.

We used the same experimental data set employed in [6] in order to evaluate the performance degradation to be accepted when sacrificing the local adaptation of the whitening filter coefficients. The reported analysis allows identifying the main limitations of the proposed approach as well as the scenarios in which it might represent a suitable solution.

The paper is organized as follows. In Section 2, we briefly recall the P-GLRT and its benefits with respect to the P-NCI. The alternative polarimetric detection scheme is described in Section 3, while Section 4 reports the experimental results obtained against the available data set. Eventually, some conclusions remarks are given in Section 5.

2 Polarimetric locally adaptive detection scheme

Let us consider a FM based PCL system, equipped with L receiving channels, connected to differently polarized surveillance antennas.

According to the polarimetric detection scheme introduced in [6], the signals collected by different antennas separately

undergo the main stages of a conventional single-channel PCL processing scheme that includes:

- (i) disturbance (direct signal and multipath) cancellation using the polarimetric version of the Extensive Cancellation Algorithm (P-ECA).
- (ii) evaluation of the Cross-Ambiguity Function (CAF) between the surveillance and the reference signal over a selected coherent processing interval (CPI).

Once these stages have been performed, L range-Doppler maps $\chi_l[r, d]$ ($l = 1 \dots L$) will be available. As is well known, beside the effectiveness of the adopted signal processing stages, a typical range-Doppler map is likely to include targets echoes as well as disturbance sources, such as thermal noise, cancellation residuals and interferences [3].

In case of $L=1$, the detection stage is typically performed by applying a Cell Average - Constant False Alarm Rate (CA-CFAR) threshold to the corresponding map in order to detect targets with a given probability of false alarm (P_{FA}).

In contrast, when multiple surveillance channels are available ($L \geq 2$), connected to differently polarized receiving antennas, different detection schemes can be considered to jointly exploit the outputs of the L channels, according to the assumptions that are made on the statistical properties of the disturbance.

Assuming that the target polarimetric characteristics might be very different from the disturbance, an adaptive detection scheme was derived in [6] by resorting to a Generalized Likelihood Ratio Test (GLRT). The corresponding detection test is given by:

$$\mathbf{x}_m^H \hat{\mathbf{D}}_m^{-1} \mathbf{x}_m \underset{H_0}{\overset{H_1}{\geq}} \lambda_{P-GLRT} \quad (1)$$

where \mathbf{x}_m is a complex vector collecting the L polarimetric outputs extracted at the m -th range-Doppler bin of the maps, λ_{P-GLRT} is a proper threshold, and $\hat{\mathbf{D}}_m$ is the estimated covariance matrix. The latter is obtained as

$$\hat{\mathbf{D}}_m = \sum_{q \in I_m} \mathbf{x}_q \mathbf{x}_q^H \quad (2)$$

where \mathbf{x}_q ($q \in I_m, |I_m| = Q$) is a set of Q secondary vectors, which contain the output of the L maps at range-Doppler locations adjacent to the Cell Under Test (CUT).

This scheme has been shown to be able to improve the target discrimination capability against the competing disturbance by exploiting the local polarimetric characteristics of the interference affecting the range-Doppler maps [6]. Specifically, this P-GLRT approach leads to several benefits with respect to a CA-CFAR detection scheme applied after a simple NCI of the outputs of the L polarimetric channels:

$$\|\mathbf{x}_m\|^2 \underset{H_0}{\overset{H_1}{\geq}} \lambda_{P-NCI} \cdot \sum_{q \in I_m} \|\mathbf{x}_q\|^2 \quad (3)$$

being λ_{P-NCI} the threshold required to obtain a given P_{FA} .

In fact, this approach was verified to yield an insufficient capability of controlling the actual false alarm rate, due to the simplifying assumption of uncorrelated disturbance at the different polarimetric channels.

However, depending on the specific application, the P-GLRT may lead to a very high computational load, since it requires repeating the estimation and the inversion of the matrix $\hat{\mathbf{D}}_m$ at each bin of the map. Therefore, a practical scheme is derived in the following by trading target detection performance for a limited computational burden.

3 Time-domain adaptive polarimetric filter

With reference to the multi-channel receiving system considered in Section 2, let us consider the L received signals after the first disturbance cancellation stage, i.e. before the CAF evaluation. By collecting the N_s samples from each polarimetric channel in the LN_s -dimensional vector \mathbf{z} , this can be written as:

$$\mathbf{z} = \boldsymbol{\alpha} \otimes \boldsymbol{\zeta}(\tau, f_{D_m}) + \mathbf{d} \quad (4)$$

where

- $\boldsymbol{\alpha}$ is a L -dimensional vector containing the unknown target amplitudes at each polarimetric channel and is assumed constant during the CPI and equal to $\mathbf{0}$ under hypothesis H_0 (disturbance only);
- $\boldsymbol{\zeta}_m = \boldsymbol{\zeta}(\tau_m, f_{D_m})$ represents the transmitted signal, delayed in time by τ_m and Doppler shifted by f_{D_m} where $[\tau_m, f_{D_m}]$ are the range-Doppler coordinates of a given target;
- \mathbf{d} is a LN_s -dimensional vector collecting the samples of the disturbance (noise, interference or cancellation residual).

Under the Gaussian assumption for the disturbance \mathbf{d} , i.e. $\mathbf{d} \sim CN(\mathbf{0}, \mathbf{M})$, and assuming a priori known the covariance matrix \mathbf{M} , a GLRT approach yields the following detector:

$$\mathbf{z}^H \mathbf{M}^{-1} (\mathbf{I}_L \otimes \boldsymbol{\zeta}_m) [(\mathbf{I}_L \otimes \boldsymbol{\zeta}_m)^H \mathbf{M}^{-1} (\mathbf{I}_L \otimes \boldsymbol{\zeta}_m)]^{-1} \underset{H_0}{\overset{H_1}{\geq}} \mu \quad (5)$$

By neglecting the temporal correlation of the disturbance sources and assuming that the polarimetric characteristics are stationary with time, we can approximate the disturbance covariance matrix with the matrix:

$$\mathbf{M} = \mathbf{D} \otimes \mathbf{I}_{N_s} \quad (6)$$

where \mathbf{D} is time-invariant polarimetric covariance matrix of the disturbance. Under this simplifying assumption, the detector in Equation (5) becomes

$$\mathbf{z}^H (\mathbf{I}_L \otimes \boldsymbol{\zeta}_m) \mathbf{D}^{-1} (\mathbf{I}_L \otimes \boldsymbol{\zeta}_m)^H \mathbf{z} \underset{H_0}{\overset{H_1}{\geq}} \mu \quad (7)$$

By observing that $\boldsymbol{\zeta}_m$ represents the matched filter to a target appearing at the m -th bin of the range-Doppler plane, we can easily state that $\mathbf{x}_m = (\mathbf{I}_L \otimes \boldsymbol{\zeta}_m)^H \mathbf{z}$.

Therefore, we notice that the detectors in Equations (7) and (1) show the same structure.

Basically, both detectors can be interpreted as the cascade of a whitening stage based on the Cholesky decomposition of matrix \mathbf{D} (i.e. $\mathbf{y}_m = \mathbf{L}^{-1}\mathbf{x}_m$ being $\mathbf{D} = \mathbf{L}\mathbf{L}^H$), followed by a NCI of the results ($\|\mathbf{y}_m\|^2 \gtrsim \mu$).

In order to make the detector in Equation (7) fully adaptive, we replace \mathbf{D} with a suitable estimate $\hat{\mathbf{D}}$. Specifically this can be obtained based on the structure of matrix \mathbf{M} in Equation (6) and assuming that the target contribution in the received data is negligible in the time domain (i.e. prior to matched filtering):

$$\hat{\mathbf{D}} = \frac{1}{N_s} \sum_{n=1}^{N_s} \mathbf{z}_n \mathbf{z}_n^H \quad (8)$$

where \mathbf{z}_n is the L -dimensional vector collecting the n -th samples of the signals received at the L polarimetric channels. Notice that, differently from the P-GLRT, the proposed approach requires the estimate and the inversion of a single covariance matrix, leading to a significantly decreased computational load. This can be further controlled by selecting the domain in which to perform the whitening stage, namely it can be applied both in time-domain and on the range-Doppler maps. Clearly, we are sacrificing the capability to adapt locally on the range-Doppler plane the coefficients of the whitening filter, which might result in a degraded target detection capability depending on the distribution of the disturbance background on that plane.

Unfortunately, the assumption in Equation (6) is unlikely to be strictly verified, and this might yield a scarce capability for the detector in Equation (7) to guarantee the CFAR property. Therefore, in order to make the detector robust to power fluctuations of the possibly un-cancelled disturbance in the range-Doppler domain, a CA-CFAR thresholding is performed after the NCI of the whitened outputs. Therefore, the overall detection scheme becomes (see Fig. 1):

$$\| \mathbf{y}_m \|^2 \underset{H_0}{\overset{H_1}{\gtrsim}} \lambda_{TD-APF} \cdot \sum_{q \in I_m} \| \mathbf{y}_q \|^2 \quad (9)$$

where \mathbf{y}_q ($q \in I_m, |I_m| = Q$) is a set of Q whitened secondary vectors extracted at range-Doppler locations adjacent to the CUT, and λ_{TD-APF} is a proper threshold.

In the following, we will refer to this detector as the Time Domain Adaptive Polarimetric Filter (TD-APF) and we will investigate its performance, aiming at understanding the impact of the considered assumption in real scenarios.

4 Experimental Results

In the performance analysis reported in this Section, we exploit the same experimental data set used in [6]. The data set consists of 2060 sequential data files, each one containing a 1.1 s registration of the signals simultaneously collected by different antennas at different carrier frequencies resulting in a total time duration of approx. 80 minutes.

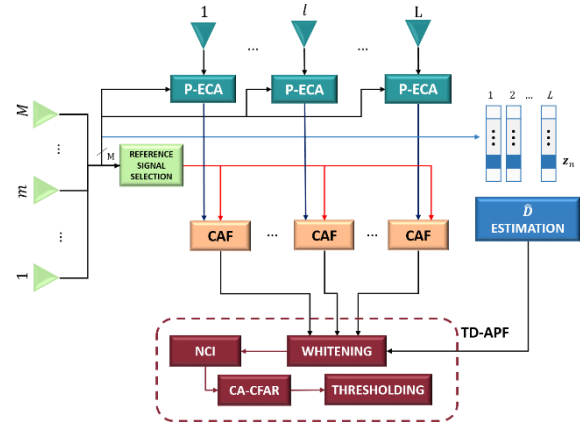


Fig. 1 Sketch of the time-domain adaptive polarimetric filter approach a FM based PCL system.

The acquisition campaign has been conducted near Fiumicino Airport, in Italy. Two receiving dual-polarized antennas have been used in the trials (see Fig. 2a). Each antenna is a three cross-elements Yagi equipped with two independent cross-polarized outputs, one vertically (V) and one horizontally (H) polarized. Specifically, one antenna was steered toward the transmitter located on Monte Cavo, approx. 25 km southeast of Rome and approx. 35 km from the receiver site, and it was employed to collect the V and H polarized versions of the reference signal. The other antenna was pointed toward the opposite direction and the two outputs gathered the V and H polarized versions of the surveillance signal. See Fig. 2b for the sketch of the acquisition geometry. The employed PCL prototype is based on a direct RF sampling approach and exploits the ICS-554 PMC module (GE Fanuc Embedded Systems).

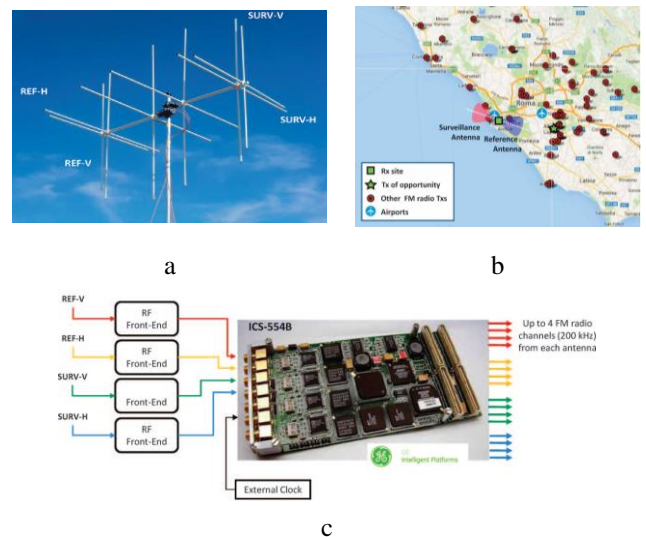


Fig. 2 Acquisition Campaign
a Sketch of multichannel passive radar prototype
b Custom-made dual-polarized antennas (three cross-elements Yagi)
c Acquisition geometry

This module consists of four 14-bit ADCs sampling synchronously the properly amplified and filtered analogue signals from up to four input channels. Simultaneous down conversion of up to 16 arbitrary signal bands (e.g. 16 FM radio channels) is provided by four Graychip GC4016 quad digital down-converters (DDC). The described setup allows collecting data from up to four different FM radio channels each one from four different antennas (see Fig. 2c).

The air-truth for the same air space has been provided by the SBS-1 real time virtual radar, a portable low-cost Mode-S/ADS-B receiver.

In order to understand the target detection performance achievable with the three polarimetric detection schemes considered above, we can compare the raw detections results provided by the employed PR receiver with the available air-truth. As an example, in Fig. 3a-c, we compare the raw detections (in green dots) provided by the system across 50 consecutive acquisitions for a single FM channel (i.e. 103.0 MHz), after the application of the P-NCI (a), the P-GLRT (b), and the TD-APF(c) detection schemes, respectively. The air-truth data are sketched in black on the same figure.

By observing Fig. 3, we can easily verify that:

- (i) the P-NCI detection scheme (Fig. 3a) offers the worst capability of controlling the false alarm rate, confirming the weakness of the assumption of statistically independent disturbance affecting the different polarimetric channels;
- (ii) the P-GLRT (Fig. 3b) and the TD-APF (Fig. 3c) approaches yield quite comparable results.

Based on the availability of real air traffic registrations, an extended detection performance analysis has been carried out by computing the performance statistics over the entire dataset.

Specifically, two kinds of results have been produced: the false alarm rate control curves and the empirical receiver operating characteristic (ROC) curves, in order to demonstrate the relative frequency of target detections against the false alarm rate parameterized by the detection threshold applied to the specific detection scheme. With respect to the detection frequency, the analysis has been limited to targets laying in the range band [0; 100] km and included within an angular sector of 90° about the surveillance antenna pointing direction. In contrast, in order to limit the impact of detections due to strong targets sidelobes and/or to targets not equipped with a transponder, the false alarm density has been recorded in the range band [150; 200] km where the target detection probability is very low so that it is expected not to affect the estimate of the false alarm rate.

In Fig. 4a-b, we report the results obtained with the three considered polarimetric approaches for the FM channel at 103.0 MHz, namely the same used for the analysis in Fig. 3. The extensive analysis confirms the behaviours observed in Fig. 3 for a small amount of consecutive scans. In fact, by observing the false alarm rate control curves in Fig. 4a, we confirm that the P-NCI detection scheme yields the worst false alarm control capability while the TD-APF approach yields almost identical performance with respect to the P-GLRT solution.

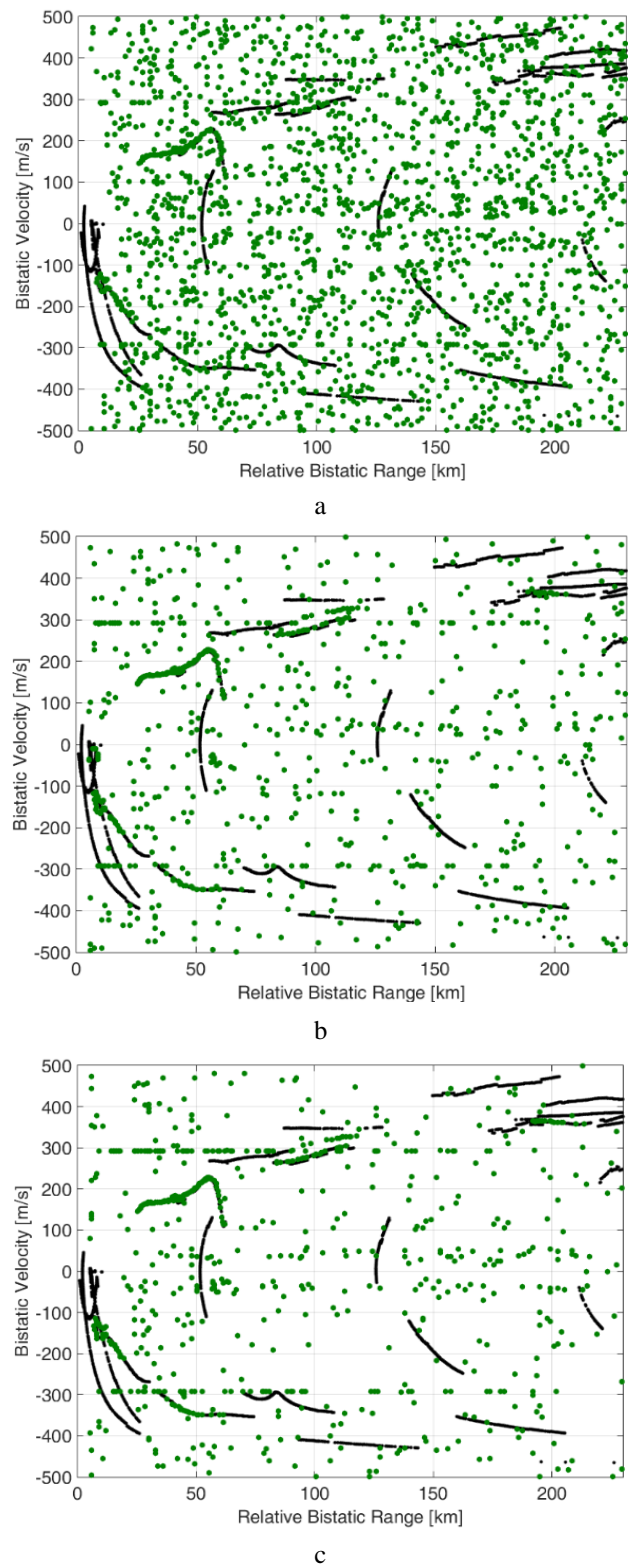
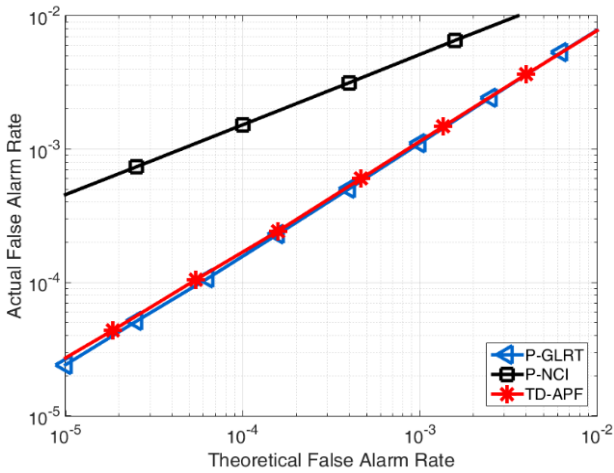
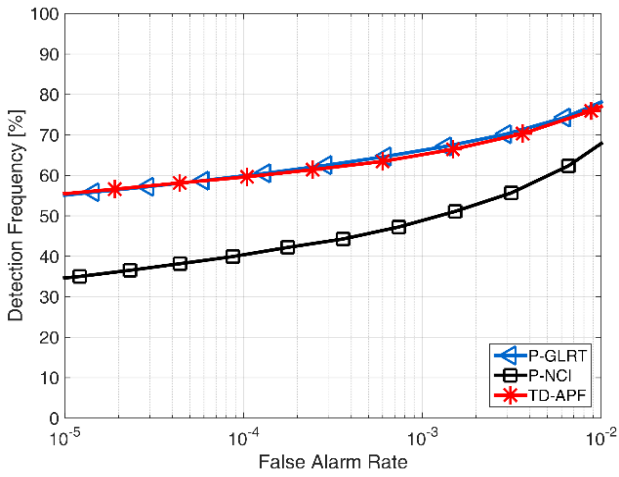


Fig. 3 Detection results for 50 consecutive acquisitions for the FM channel at 103.0 MHz using
a P-NCI
b P-GLRT
c TD-APF



a



b

Fig. 4 Performance analysis using different approaches for the FM channel at 103.0 MHz
 a Actual false alarm rate vs nominal false alarm rate curves
 b Empirical ROC curves

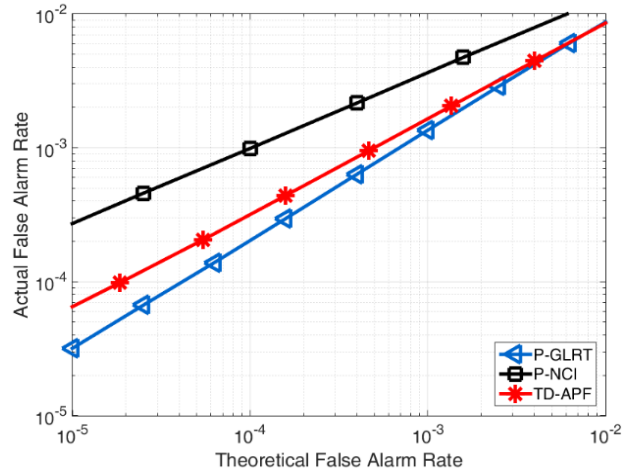
Similarly, by observing the ROC curves in Fig. 4b, we see that the TD-APF approach yields comparable results with respect to the P-GLRT. Hence, we can assume that, at this particular FM channel, the disturbance was such that it did not require a localized adaptation. Moreover, it is apparent that the detection capability improvement that both the adaptive approaches offer is tremendous with respect to the simple P-NCI.

In fact, the latter suffers from the impossibility of counteracting the disturbance in the polarimetric domain and only relies on the capability to integrate the target echoes at differently polarized antennas. Similar conclusions have been drawn when exploiting the signals for other two out of the three available FM radio channels (the results are not reported here for the sake of brevity).

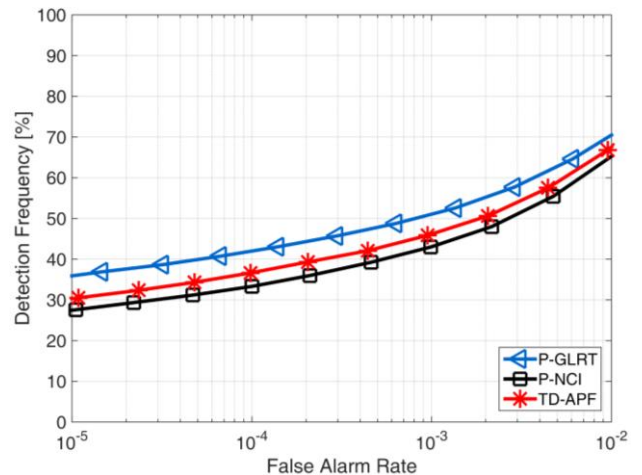
However, this is not a general result. In fact, when the FM channel at 91.2 MHz is considered, some differences are observed.

In Fig. 5a-b we report the false alarm rate control curves and the ROC curves for the aforementioned FM channel. In this case, as is apparent by observing Fig. 5a, the false alarm control capability offered by the TD-APF is slightly worse with respect to the P-GLRT. Still, the TD-APF offers a considerably better false alarm control with respect to the P-NCI. Moreover, the target detection performance (see Fig. 5b) of the TD-APF approach is no longer comparable to the P-GLRT detection scheme, showing that the simplified assumptions on the polarimetric characteristics of the disturbance are not valid at this channel.

However, it is worth noticing that, for this specific frequency channel, even the P-GLRT offers a small improvement in terms of detection capability with respect to the simple P-NCI. This result possibly reveals that the exploitation of polarimetric diversity is not very useful in this case.



a



b

Fig. 5 Performance analysis using different approaches for the FM channel at 91.2 MHz
 a Actual false alarm rate vs nominal false alarm rate curves
 b Empirical ROC curves

5 Conclusions

In this paper, we presented a practical approach for a polarimetric adaptive detection scheme to be employed in passive radar systems. Based on simplifying assumptions on the disturbance limiting the detection performance of the PCL system, the proposed approach allows limiting the computational complexity with respect to previously proposed detections schemes. Specifically, the lower cost approach requires the estimation and the inversion of a single disturbance covariance matrix at each coherent processing interval, resulting in a global estimate of the adaptive weights of the polarimetric withering filter. The analysis conducted against experimental data revealed that the above assumptions do not yield a significant loss in terms of achievable performance in many cases, especially when the adaptive exploitation of the polarization diversity is found to be essential for enhancing the target detection capability of the system.

References

- [1] P.E., Howland, IEE Proc. Radar, Sonar and Navigation. (Special Issue on Passive Radar System), 152, 3, (June 2005)
- [2] P. Lombardo, F. Colone: "Advanced processing methods for passive bistatic radar", in W.L.Melvin and J. A.Scheer (Eds):"Principles of Modern Radar: Advanced Radar Techniques", Raleigh,NC: SciTech Publishing, pp. 739–82, (2012)
- [3] H. Griffiths, C. Baker: "The signal and interference environment in passive bistatic radar", Proceedings of IEEE IDC 2007, Adelaide, Australia, February 2007
- [4] C. Bongioanni, F. Colone, T. Martelli, R. Angeli, P. Lombardo, "Exploiting polarimetric diversity to mitigate the effect of interferences in FM-based passive radar", Proceedings of 11th International Radar Symp., Vilnius (LT), June 2010.
- [5] J. You, X. Wan, Y. Fu, G. Fang: "Experimental study of polarisation technique on multi-FM-based passive radar", IET Radar, Sonar & Navigation, 9, 7, pp. 763-771, (2015).
- [6] F.Colone, P.Lombardo:"Polarimetric passive coherent location", IEEE Transactions on Aerospace and Electronic Systems, 51,2, pp.1079–97, (2015).
- [7] M. Conti, C. Moscardini, A. Capria, "Dual-polarization DVB-T passive radar: Experimental results", Proc. IEEE Radar Conf 2016, Philadelphia, (PA), May 2016, pp. 1-5.
- [8] F. Filippini, F. Colone, D. Cristallini, G. Bournaka: "Experimental results of Polarimetric Detection Schemes for DVB-T based Passive Radar", IET Radar Sonar and Navigation, 2017, in press